A novel nanozyme assay utilising the catalytic activity of silver nanoparticles and SERRS

S. Sloan-Dennison [a], S. Laing [a], N. Shand [b], D. Graham [a] and K. Faulds [a]

Artificial enzymes have become an increasingly interesting area of research due to their many advantages over natural protein enzymes which are expensive, difficult to isolate and unable to stand harsh environments. An important area of this research involves using metal nanoparticles as artificial enzymes, known as nanozymes, which exhibit peroxidase-like activity enabling them to catalyse the oxidation of substrates such as 3,3',5,5'-tetramethylbenzidine (TMB) in the presence of hydrogen peroxide (H_2O_2), giving a colorimetric response. Here we exploit the catalytic activity of silver nanoparticles (Ag NPs) in a surface based silver-linked immunosorbent assay (SLISA) to detect human C-reactive protein (CRP), an inflammatory marker. Ag NPs were conjugated to antibodies with specific recognition for the corresponding target antigenic molecule, CRP, and the Ag NPs were used to catalyse the oxidation of TMB by H_2O_2. The resulting coloured oxidation product was detected using SERRS. We demonstrate that Ag NPs can replace the enzymes used in a conventional ELISA and a detection limit of 1.09 ng/mL of CRP can be achieved. It indicates the promise for SLISAs for biomarker detection and opens the way for further assays of this nature to be created. This novel assay has the potential to be optimised to detect lower levels of CRP and can be further extended for the sensitive and specific detection of other relevant biomarkers.

Introduction

C-reactive protein (CRP) is a pentameric protein which is found in blood plasma and is a systemic marker of inflammation and tissue damage.[1] Although it is considered a non-specific biomarker, research has suggested that patients with an elevated base level of CRP are at a higher risk of diabetes,[2] sepsis,[3] and most importantly, cardiovascular disease.[4] Thus, monitoring CRP levels is considered a useful method of screening and disease management. CRP is conventionally detected using an enzyme-linked immunosorbent assay (ELISA), which is a commonly employed clinical method for the detection and quantification of biomarkers. Sandwich ELISAs utilise a monoclonal antibody immobilised on a solid substrate with specificity for a distinct antigen. Following the specific antibody-antigen interaction, a secondary antibody can be added, which is functionalised with an enzyme.[5] The enzyme activity can subsequently be measured by means of its reaction with a chromogenic substrate, such as 3,3',5,5'-tetramethylbenzidine (TMB), which is oxidised to a blue charge transfer complex (CTC). This then generates a detectable colorimetric signal which is proportional to the amount of analyte present. Therefore, by measuring the intensity of the blue colour of the CTC using UV-vis spectroscopy, the concentration of target can be determined.

Resonance Raman spectroscopy (RRS) has also been utilised in combination with TMB for detection in a standard ELISA by using a Raman excitation wavelength in resonance with the absorbance maxima of the CTC.[6] In this approach, it was demonstrated that by using RRS in place of the traditional colorimetric detection method, a 50 times lower detection limit of antigen (TNF-α) was achieved. This method was also extended to a surface-based assay for the detection of prostate-specific antigen (PSA) with a detection limit of 60 ng/mL. [7]

To further increase the sensitivity, nanoparticles (NPs) have also been incorporated into ELISAs. Merkoci et. al. first demonstrated the use of gold (Au) NPs as carriers of signalling antibody, functionalised with the enzyme horseradish peroxidase (HRP), in order to achieve amplification of the signal.[8] Since the Au NPs allow more HRP to be present per antigen-antibody interaction, more HRP-mediated TMB oxidation can take place. Therefore, when analysed using UV-vis

a. *Centre for Molecular Nanometrology, Technology and Innovation Centre, University of Strathclyde, 99 George Street, Glasgow, UK*
b. *DSTL, Porton Down, Salisbury UK,*

spectroscopy, an enhanced oxidation signal was obtained. Another benefit of using NPs in ELISAs is the ability to utilise their roughened metal surface by adsorbing colorimetric probes onto them and analysing using surface enhanced resonance Raman scattering (SERRS) which was first reported by Campbell et al.[9] When the ELISA substrate bromochloroindolylphosphate (BCIP), was added to the sandwich ELISA with an antibody conjugated to alkaline phosphate, a blue dimeric species was produced which could be adsorbed onto Au NPs and a strong SERRS signal was achieved and correlated to the concentration of CRP. Graham et. al. also reported the use of SERRS as a readout technique in an ELISA by using the commercially available peroxidase substrate 2,2'- azino-bis (3-ethylbenzothiazoline-6-sulphonic acid) (ABTS), as the enzyme-transformable chromogen.[10] Detection antibody functionalised with HRP was used to oxidise the ABTS and upon the addition of Au NPs, the oxidised ABTS was adsorbed onto the surface. SERRS analysis could take place by interrogating the solution using a laser with an excitation wavelength close to the absorbance maximum of the oxidised ABTS product and could detect pg/mL detection of prostate specific antigen. More recently silver (Ag NPs) have been used to increase the signals obtained from an ELISA. Zhan et al. reported the electrostatic attraction of negatively charged citrate capped Ag NP to the positively charged oxidised TMB product of an ELISA.[11] Aggregation of the Ag NP was also induced, producing highly enhanced Raman scattering which could be related to the concentration of respiratory syncytial, resulting in pg/mL detection.

All of these ELISAs used detection antibodies conjugated to HRP due to its effectiveness in catalysing the oxidation of TMB. However, its enzymatic activity gradually decreases with its long term storage and the isolation of HRP is time consuming and expensive.[12] Therefore, there has been a significant interest into the investigation of NPs as artificial enzymes, known as nanozymes, due to their cheap and easy synthesis, long term storage, robustness in a variety of environments and size/composition dependent activity which could address the disadvantages of natural enzymes.[13]

Recently, it has been found that many metal NPs possess an intrinsic enzyme mimetic activity. The first example of this activity was reported by Gao et. al.[14] in 2007, who showed that ferromagnetic nanoparticles (MNPs) exhibit is catalytic activity and can catalyse the oxidation of TMB in the presence of hydrogen peroxide (H_2O_2). The catalytic activity of MNPs was also developed into a capture-detection sandwich immunoassay format for a simple colorimetric assay, to detect the presence and concentration of rotavirus by measuring the intensity of the blue CTC produced by the MNPs.[15] This intrinsic enzyme mimetic activity is not restricted to MNPs and there has been a recent rise in publications describing a variety of metal NPs with catalytic activity, including ceria,[16] Au [17] and Ag NPs,[18] all of which have been used for the detection of glucose and/or H_2O_2. Furthermore, many research groups have investigated and adopted the classic sandwich immunoassay format for detection using many different peroxidase mimicking nanozymes. For example, Kim et. al. utilised the highly active peroxidase mimics, MNPs and platinum NPs, within porous carbon, as a signalling element for labelling with

antibodies for the detection of human epidermal growth factor with a detection limit as low as 1.5 ng/mL when analysed using UV-vis spectroscopy. [19] The catalytic activity of Au NPs conjugated to antibodies has also been applied in an ELISA format. However, Wang et al. reported that the catalytic activity was inhibited due to the addition of the protein molecules, but could be increased by the deposition of Au due to the formation of a new Au shell. When added, TMB was oxidised producing a bright blue colour and a naked eye limit of detection (LOD) of 5 ng/mL of human immunoglobulin (IgG) was achieved. The catalytic activity of Au NP conjugated to antibodies has also been increased by combining them with carbon nanotubes, and the resulting nanohybrid displayed enhanced catalytic activity.[20]

The enzyme mimicking activity of Ag NPs has also been demonstrated to catalyse the oxidation of TMB with H_2O_2. However, unlike other nanozymes, the oxidised CTC product can be detected not only by UV-vis spectroscopy but also by SERRS. Recently we have shown that the catalytic activity of Ag NPs can be used to provide a novel method of analysis for the detection of H_2O_2.[18] The Ag NPs catalyse the oxidation of TMB to the resulting positively charged CTC, which was adsorbed onto the surface of the Ag NPs resulting in a SERRS response. This approach of applying SERRS for the detection of the nanozyme-catalysed oxidation product resulted in the fast, direct detection of H_2O_2 with a detection limit of 100 nM.[18]

In the work reported here, we investigate the combination of an ELISA with the novel concept of utilising the peroxidase properties of
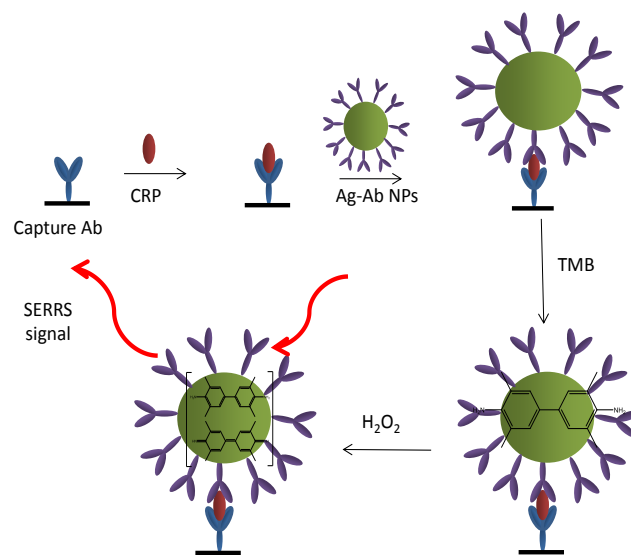

Fig.1 Schematic of SERRS detection of CRP using a SLISA. Capture antibodies were immobilised onto the surface of a nitrocellulose coated glass slide, followed by incubation with CRP and silver nanoparticles functionalised with antibody (Ag-Ab NP's). TMB and H_2O_2 were then added and the Ag NP's catalyse the oxidation of TMB to the CTC, which can then be detected using SERRS.

Ag NPs, enabling the sensitive detection using SERRS, without increasing the complexity of the procedure in this first in class immunoassay. We demonstrate the application of Ag NPs conjugated to antibodies, which can replace conventional enzymes such as HRP, therefore the Ag NPs acts as an enzyme mimic, for the detection of CRP, creating a silver-linked immunosorbent assay (SLISA) shown in Figure 1. By introducing Ag NPs into the assay, the TMB is oxidised without the need of an enzyme conjugated to an antibody, therefore reducing the cost of the assay. The coloured oxidised TMB product can also be analysed using SERRS and a lower detection limit of CRP can be achieved.

Experimental

Materials

Silver nitrate, sodium citrate, 3,3',5,5'-tetramethylbenzidine (TMB), hydrogen peroxide, Tween 20® and phosphate-buffered saline (PBS) tablets were all purchased from Sigma Aldrich, UK. TMB blotting solution was purchased from Thermo Fisher Scientific, UK. An ELISA test kit comprising of capture antibody and CRP standard was purchased from R&D systems, UK, PATH® protein microarray slides were purchased from GRACE bio-labs, USA and SeraSub was purchased from CST Technologies, USA.

Instrumentation

Extinction measurements were all carried out using a Cary 300 Bio UV-vis spectrometer. Particle size and zeta measurements were obtained using a Malvern Zetasizer Nano series. Solution spectra were collected using a Snowy Range Sierra series reader with a 638 nm excitation wavelength with a 4.5 mW laser power. Raman spectra from nitrocellulose surfaces were collected using a Renishaw InVia microscope with a 633 nm excitation wavelength with 0.8 mW laser power. The solution measurements were used to optimise the NP functionalisation conditions and the 633 nm microscope system was used for detection in the final assay.

Silver nanoparticle synthesis and characterisation

All glassware was soaked in aqua regia (HCl, HNO_3 3:1 v/v) for 1-2 hours before use. 500 mL of distilled water was heated to 45 °C in a 3 necked round bottom flask. 90 mg of silver nitrate (dissolved in 10 mL of distilled water) was then added and the solution heated until boiling. A 10 mL solution of 1% sodium citrate was then added and boiling maintained for 90 minutes. Constant stirring was maintained throughout using a glass linked stirrer. The synthesised Ag NPs were characterised using extinction spectroscopy to obtain the maximum absorbance by diluting 50 µL in 450 µL of distilled water. The concentration of the Ag NPs could then be calculated using the Beer-Lambert law and a molar extinction coefficient of

1.04×10^{10} M^{-1} cm.[21] Size and zeta measurements were obtained by analysing 1 mL of the colloidal nanoparticles on a Malvern Zetasizer. (See supplementary information Figure 1).

Catalytic activity of Ag NPs

100 µL of Ag NPs (0.8 nM) was added to 100 µL of TMB (3 mM), 100 µL of H_2O_2 (6 mM) and 200 µL distilled water and analysed using extinction spectroscopy by taking 50 µL of the sample and diluting it in 450 µL distilled water and with Raman spectroscopy, with no dilution, using a 638 nm laser excitation at 40 mW and a 1 second accumulation time. Control samples were carried out by omitting one of the components of the assay and were also analysed in the same manner, replacing the omitted components with distilled water in each case. Samples were prepared in triplicate and 5 scans of each were obtained.

Functionalisation of Ag-Ab NP conjugates

Final concentrations of mouse anti-human CRP antibody (2.5, 1, 0.5, 0.25, 0.05 and 0 µg/mL) were added to 1 mL of Ag NPs with a pH of 7.9 and left to shake overnight. The solutions were then centrifuged, the supernatant removed and the NPs resuspended in 500 uL of distilled water. Ag-Ab NPs were then characterised using extinction spectroscopy and dynamic light scattering (DLS) (See supplementary information Figure 2 (a) and (b)).

Catalytic activity of Ag-Ab NPs

100 µL of Ag-Ab NPs conjugate was added to 100 µL of TMB (3 mM), 100 µL of H_2O_2 (6 mM) and 200 µL of distilled water and analysed with a 638 nm laser excitation at 40 mW and a 1 second accumulation time. Samples were prepared in triplicate and 5 scans of each were obtained.

Silver-linked immunosorbent assay (SLISA)

0.3 µL of mouse anti-human CRP antibody (10 µg/mL) was spotted onto a nitrocellulose coated glass slide and left to incubate overnight at room temperature. The slide was then washed three times with wash buffer (0.05% Tween 20® in PBS buffer (pH 7.4)) and 20 µL of human CRP (various concentrations) was then added and left to incubate for 20 minutes, followed by three wash steps with wash buffer. 20 µL of Ag-Ab NP conjugates was then added to the slide and left to incubate for 15 minutes before washing again. 20 µL of TMB blotting solution was then added and removed after 20 minutes followed by a final wash step with wash buffer.

SLISA controls were also performed using 25 ng/mL of bovine serum albumin (BSA) and Human chronic gonadotropin (hCG). The SLISA was also carried out using 1% seraSub spiked with 100 ng/mL CRP.
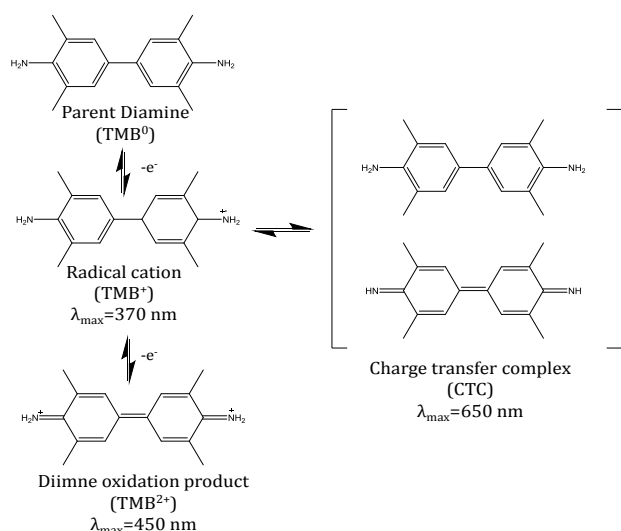
Fig.2 Oxidation of TMB by H_2O_2 in the presence of Ag NPs to its first oxidation step (TMB+), which exists in equilibrium with the charge transfer complex (CTC), and to the second oxidation step (TMB2+) with the addition of an acid.

SERRS analysis

The SLISA was analysed as follows: each SLISA spot (with different concentrations of CRP) was interrogated at 100 different random points using a 633 nm laser excitation with a 9 second accumulation time and 0.8 mW laser power. The spectra were then baseline corrected using intelligent fitting on WiRE 4.2 software and the overall spot average was obtained using Matlab
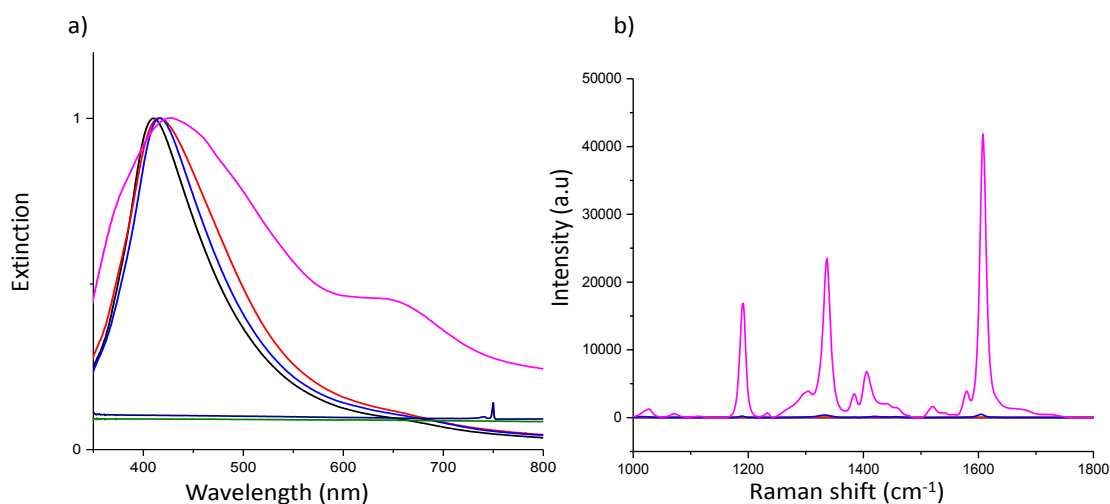
Results and discussion

As shown in Figure 1, detection antibodies functionalised with enzymes that are used in traditional ELISAs can be replaced with citrate capped Ag NPs functionalised with antibody, to form a SLISA. When capture antibody and CRP are immobilised onto a solid substrate, Ag NPs conjugated to antibodies can specifically bind to the immobilised CRP forming the SLISA spot. Once TMB is added, the Ag NPs catalyse the oxidation with H_2O_2 and the oxidised TMB can be detected using SERRS. The intensity of the oxidised TMB signal can therefore be related to the concentration of Ag NPs, which can be correlated to the amount of CRP present.

Catalytic activity of Ag NPs

The oxidation of TMB by Ag NPs and H_2O_2 occurs via the two-step two-electron oxidation shown in Figure 2. The first one-electron oxidation produces a radical cation with an absorbance maximum at 370 nm, which exists in equilibrium with the blue CTC which has an absorbance maximum at 650 nm. The addition of a strong inorganic acid then terminates the reaction yielding the yellow TMB^{2+} with an absorbance maximum at 450 nm. [22]

To demonstrate the oxidation of TMB via the catalytic activity of Ag NPs, Ag NPs (0.8 nM) were added to TMB (3 mM) and H_2O_2 (6 mM) and the extinction spectrum (along with spectra from control experiments) are shown in Figure 3 (a). The oxidation of the TMB is clearly visible by the appearance of the absorption maximum of the CTC at 650 nm when TMB and H_2O_2 were added. This peak does not appear in any of the control experiments confirming the catalytic activity of Ag NPs. Aggregation also occurred when all three components were added due to the positive CTC molecule being formed, which is electrostatically attracted to the negative NP surface, effectively pulling multiple NPs together.

Fig. 3 (a) Normalised extinction spectra and (b) SERRS response of H_2O_2 (green), TMB (dark blue), Ag NPs (black), Ag NPs and H_2O_2 (red), Ag NPs and TMB (light blue) and Ag NPs, TMB and H_2O_2 (pink). Extinction spectra were normalised to 1 for clarity and SERRS spectra were obtained using a 638 nm laser excitation with a 1 second accumulation time and 4.5 mW laser power. The spectra shown are the average of 5 measurements of 3 replicate samples

The SERRS results obtained, shown in Figure 3 (b), confirmed that TMB is only oxidised to the CTC in the presence Ag NPs and H_2O_2. The spectrum shows the three main characteristic peaks of the CTC, 1191 cm^{-1}, 1336 cm^{-1} and 1610 cm^{-1}, which represent CH_3 bending modes, inter-ring C-C stretching modes and a combination of ring-stretching and CH bending modes, respectively.[18] A small CTC signal occurs when just TMB is added to the Ag NPs due to H^+ ions on the surface of the NP causing some oxidation of the TMB.

The catalytic activity of the Ag NPs is proposed to be attributed to the adsorption of H_2O_2 on the surface of Ag NPs, causing it to break into OH radicals as the Ag NP surface is oxidised from Ag^0 to Ag^+. The free radicals then proceed to cause the oxidation of the TMB to the CTC, forming H_2O in the process.[23] Therefore, as the catalytic activity is dependent on the initial adsorption of H_2O_2, the catalytic activity of Ag NPs is high due to its un-functionalised citrate capped surface. For this reason, it was unknown whether Ag NPs functionalised with antibodies would exhibit the same catalytic property since a large portion of the Ag NP surface will no longer be available, which could adversely affect the oxidation of TMB by the metal surface.

To investigate the effect of surface modification on the catalytic activity, Ag NPs were functionalised with mouse anti-human CRP antibody. Final concentrations of 2.5, 1, 0.5, 0.25 and 0.05 µg/mL were added to the Ag NPs via a pH correction method. By altering the pH of the antibodies to lower than their amine pKa, the antibodies became positively charged and could therefore electrostatically bind to the negative Ag NP surface, creating Ag-Ab NP conjugates. 3 mM TMB and 6 mM H_2O_2 were added to the Ag-Ab NP conjugates and then analysed using 638 nm laser excitation to

Fig. 4 SERRS spectra of CTC when Ag-Ab NP conjugates (2.5 (dark blue), 1 (green), 0.5 (pink), 0.25 (blue) and 0.05 (red) and 0 (black) µg/mL of antibody) were added to TMB and H_2O_2. SERRS spectra were obtained using a 638 nm laser excitation with a 1 second accumulation time and 4.5 mW laser power. The spectra shown are the average of 5 measurements of 3 replicate samples.

assess the catalytic activity.

When high concentrations of antibody (2.5 µg/mL and 1 µg/mL) were functionalised to the Ag NP surface and TMB and H_2O_2 added, little TMB oxidation was observed which was evident in the weak CTC spectra obtained. As the concentration of antibody on the surface decreased, a more intense CTC spectrum was obtained, indicating that more oxidation had occurred. This was expected as antibodies, which are roughly 150 KDa in size, take up a lot of space on the Ag NP, significantly reducing the surface area of the Ag metal available to partake in the decomposition of H_2O_2. This resulted in less TMB becoming oxidised and a lower concentration of CTC molecules being electrostatically attracted to the surface and experiencing SERRS enhancement. The lowest concentration of antibody on the Ag NP surface (0.05 µg/mL) gave the most TMB oxidation after the Ag NP's; however, it was not chosen to be used in the SLISA as the bare Ag NP surface could potentially give rise to non-specific binding. Therefore, Ag NPs with 0.5 µg/mL of antibody on the surface were used in the subsequent SLISA, since there was enough antibody to detect CRP and prevent non-specific binding with sufficient surface area of the Ag metal remaining available for TMB oxidation.

Silver-linked immunosorbent assay

Ag-Ab NPs were then employed in the SLISA for the detection of CRP, replacing the conventional enzyme linked detection antibody. The assay was performed on nitrocellulose coated glass slides encased in a microarray chamber to allow separation of samples into individual wells. 0.3 µL of 10 µg/mL CRP-specific capture antibody was immobilised onto the nitrocellulose coated glass, electrostatically attaching them to the surface. The antibodies were left to incubate overnight to allow full immobilisation. The resulting antibody spots were then washed with 0.05 % Tween 20® in PBS (at pH 7.6) three times to remove any unbound antibody. 20 µL of CRP was then added to each antibody spot and bound to the immobilised antibodies. Further wash steps occurred followed by the addition of Ag-Ab NPs which completed the SLISA by binding to the CRP. The assay was then washed, leaving an Ag-Ab NP residue on the spot where the capture antibody had originally been deposited. Finally, TMB blotting solution (a solution of premixed TMB and H_2O_2) was added and the immobilised Ag-Ab NPs were able to oxidise the TMB in the presence of H_2O_2. Upon removal of the TMB blotting solution, the positive oxidised TMB was left bound to the Ag surface. A final wash step ensured that only the CTC electrostatically attached to the Ag NP surface was left behind.

The SLISA was performed with varying concentrations of CRP and the resulting oxidised TMB was analysed using 633 nm laser excitation. Each spot was interrogated at 100 different areas for 9 seconds each time to achieve an average CTC spectrum for each concentration of CRP added to the SLISA. The resulting average spectra of oxidised TMB obtained for each CRP concentration are shown in Figure 5 (a).

It can be observed in Figure 5 (a), that the intensity of the oxidised CTC decreases as the concentration of CRP is lowered. This is due to there being a lower concentration of Ag-Ab NPs bound to the SLISA when there is a lower concentration of CRP to bind to. The
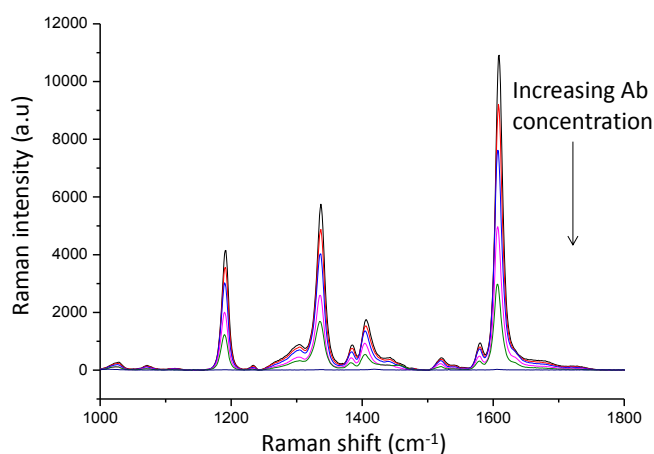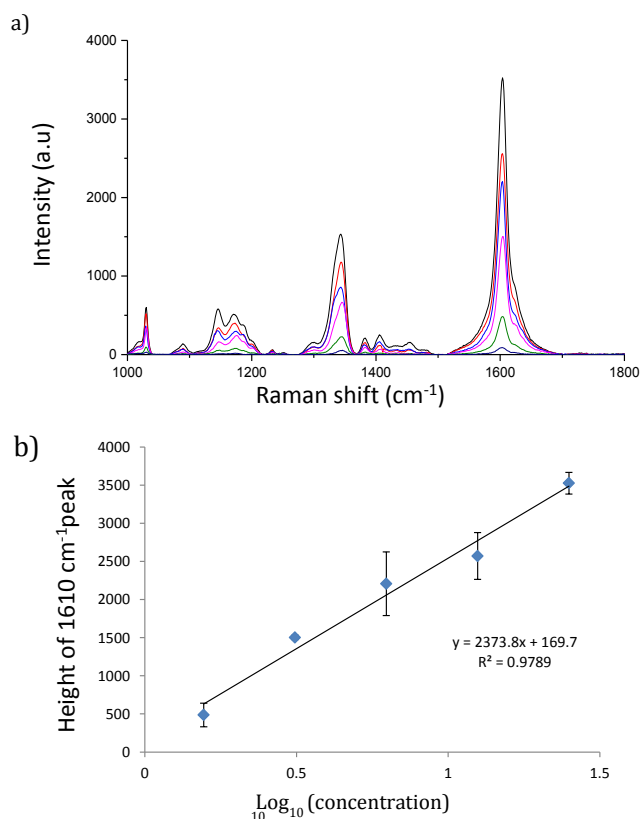
a)

b)

Fig. 5 (a) SERRS response from each SLISA spot obtained when different concentrations of CRP were added (25 (black), 12.5 (red), 6.25 (blue), 3.125 (pink), 1.56 (green) and 0 (dark blue) ng/mL of CRP). SERRS spectra were collected using a 633 nm laser excitation with a 9 second accumulation time and 0.8 mW laser power. (b) Plot of intensity of 1610 cm^{-1} peak against the Log_{10} of the CRP concentration showing linear relationship in the concentration range of 1.56-25 ng/mL (coefficient of determination, R=0.98). Errors bars indicate standard deviation from 3 replicates with 100 measurements on each taken.

appearance of the small extra peaks in the CTC spectrum at 1031, 1147, 1175 and 1623 cm^{-1} have been attributed to coming from components used in the wash and from the nitrocellulose surface itself being enhanced by the Ag NPs; however, they can be disregarded as they do not interfere with the overall CTC spectrum.

The height of the 1610 cm^{-1} peak was plotted against the logarithm to base 10 of the CRP concentration and a satisfying linear relationship was observed (over the range of 1.56-25 ng/mL) with a correlation coefficient of 0.98 as shown in Figure 5 (b). The limit of detection was calculated using 3 times the standard deviation of the blank divided by the gradient of the line and was found to be 1.09 ng/mL. The relative standard deviations were calculated using the three repeats of each concentration performed in the SLISA and the average relative standard deviation of the whole SLISA was calculated to be 13.95% indicating good reproducibility of the assay

The ensure the SLISA was only selective for CRP, control experiments were carried out to ensure the response was CRP specific. 25 ng/mL of bovine serum albumin (BSA), Human chronic gonadotropin (hCG) or CRP was added to immobilised capture antibody, followed by Ab-Ag NPs and TMB blotting solution. The SLISA spots were analysed and the resulting average SERRS intensity of the 1610 cm^{-1} of the oxidised TMB SERRS spectra obtained for each CRP, BSA and hCG are shown in the bar graph in Figure 6 (a). As an oxidised TMB signal was only obtained when CRP was present this confirmed the selectivity of the SLISA which gave no false positives from interfering biomolecules.

The SLISA was also performed to detect a clinically relevant concertation of CRP in serum to demonstrate its potential for the detection of clinical samples. 1% SeraSub spiked with 100 ng/mL of CRP was added to immobilised capture antibody with 1% SeraSub acting as a blank, followed by Ab-Ag NPs and TMB blotting solution.

The SLISA spots were analysed and the resulting average intensity of the 1610 cm^{-1} peak of the oxidised TMB SERRS spectra obtained and the results are shown in Figure 6 (b). TMB was only oxidised when CRP was present, therefore CRP could be detected using SLISA in serum samples equating to 10 μg/mL of CRP in 100% serum, which is a clinically relevant concentration which would indicate inflammation in the body.[24]

Conclusion

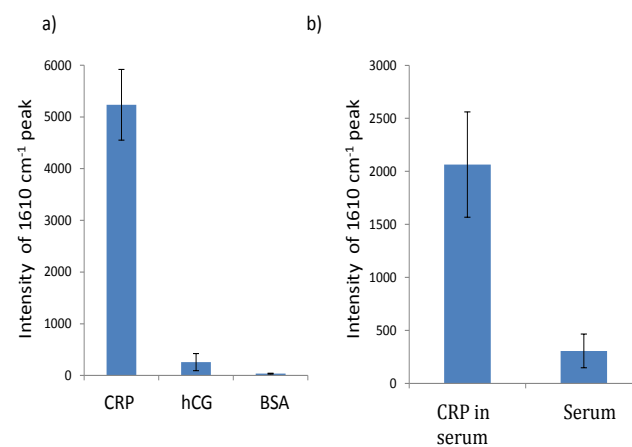a)   b)

Fig. 6 (a) Bar graph of the SERRS intensity of the 1610 cm^{-1} peak of oxidised TMB signal produced from the SLISA performed with CRP, hCG and BSA. (b) Bar graph of the intensity of the 1610 cm^{-1} peak of oxidised TMB signal produced from the SLISA performed in 1% serum spiked with 100 ng/mL and 1% serum. Errors bars indicate standard deviation from 3 replicates with 100 measurements on each taken.

This work reports the first use of the inherent peroxidase-like activity of Ag NPs in an ELISA format. We have shown that Ag-Ab NPs can be used to replace antibodies conjugated to conventional enzymes used in an ELISA by catalysing the oxidation of TMB in the presence of H_2O_2. We have also demonstrated that the SLISA can be analysed

using SERRS by utilising the roughened surface of the Ag NPs in combination with a laser in resonance with the absorbance maxima of the oxidised TMB. This has allowed for the novel detection of CRP with a calculated detection limit of 1.09 ng/mL., which is comparable to LODs that have been achieved using fluorescence, [25] colorimetric,[26] and electrochemical detection[26] which have reported detection limits of between 1-2 ng/mL. The SLISA also showed good selectivity and the practicality was demonstrated by detecting CRP in a biological matrix.

Another advantage of the SLISA over the conventional ELISA is the decrease in incubation time required for a positive result (20 minute incubation of each component as opposed to 2 hours), allowing the SLISA to be completed and analysed in a matter of hours instead of a whole day.

Since this method is simply transferrable to almost any target analyte, the SLISA has the potential to be applied for the sensitive and specific detection of a variety of relevant biomarkers for the detection and diagnosis of disease

Acknowledgements

References

1. A. K. Shrivastava, H. V. Singh, A. Raizada and S. K. Singh, *The Egyptian Heart Journal*, 2015, **67**, 89-97.
2. Y. Doi, Y. Kiyohara, M. Kubo, T. Ninomiya, Y. Wakugawa, K. Yonemoto, M. Iwase and M. Iida, *The Hisayama Study*, 2005, **28**, 2497-2500.
3. G. P. Castelli, C. Pognani, M. Meisner, A. Stuani, D. Bellomi and L. Sgarbi, *Critical Care*, 2004, **8**, R234.
4. A. M. Wilson, M. C. Ryan and A. J. Boyle, *International Journal of Cardiology*, 2006, **106**, 291-297.
5. R. M. Lequin, *Clinical Chemistry*, 2005, **51**, 2415-2418.
6. S. Laing, A. Hernandez-Santana, J. Sassmannshausen, D. L. Asquith, I. B. McInnes, K. Faulds and D. Graham, *Analytical Chemistry*, 2011, **83**, 297-302.
7. S. Laing, E. J. Irvine, A. Hernandez-Santana, W. E. Smith, K. Faulds and D. Graham, *Anal. Chem.*, 2013, **85**, 5617-5621.
8. A. Ambrosi, F. Airò and A. Merkoçi, *Analytical Chemistry*, 2010, **82**, 1151-1156.
9. F. M. Campbell, A. Ingram, P. Monaghan, J. Cooper, N. Sattar, P. D. Eckersall and D. Graham, *Analyst*, 2008, **133**, 1355-1357.
10. R. Stevenson, A. Ingram, H. Leung, D. C. McMillan and D. Graham, *Analyst*, 2009, **134**, 842-844.
11. L. Zhan, S. J. Zhen, X. Y. Wan, P. F. Gao and C. Z. Huang, *Talanta*, 2016, **148**, 308-312.
12. X. Wang, Y. Hu and H. Wei, *Inorganic Chemistry Frontiers*, 2016, **3**, 41-60.
13. J. Liu, X. Hu, S. Hou, T. Wen, W. Liu, X. Zhu and X. Wu, *Chemical Communications*, 2011, **47**, 10981-10983.
14. T. WANG, J. FENG, D. YANG, S. PERRETT and X. YAN, 2007.
15. M.-A. Woo, M. Kim, J. Jung, K. Park, T. Seo and H. Park, *International Journal of Molecular Sciences*, 2013, **14**, 9999.
16. X. Jiao, H. Song, H. Zhao, W. Bai, L. Zhang and Y. Lv, *Analytical Methods*, 2012, **4**, 3261-3267.
17. Y. Jv, B. Li and R. Cao, *Chemical communications (Cambridge, England)*, 2010, **46**, 8017-8019.
18. K. S. McKeating, S. Sloan-Dennison, D. Graham and K. Faulds, *Analyst*, 2013, **138**, 6347-6353.
19. M. I. Kim, Y. Ye, M.-A. Woo, J. Lee and H. G. Park, *Advanced Healthcare Materials*, 2014, **3**, 36-41.
20. S. R. Ahmed, J. Kim, T. Suzuki, J. Lee and E. Y. Park, *Biosensors & bioelectronics*, 2016, **85**, 503-508.
21. J. Yguerabide and E. E. Yguerabide, *Analytical biochemistry*, 1998, **262**, 137-156.
22. P. D. Josephy, T. Eling and R. P. Mason, *Journal of Biological Chemistry*, 1982, **257**, 3669-3675.
23. C. K. Tagad, H. U. Kim, R. C. Aiyer, P. More, T. Kim, S. H. Moh, A. Kulkarni and S. G. Sabharwal, *RSC Advances*, 2013, **3**, 22940-22943.
24. M. Fröhlich, A. Imhof, G. Berg, W. L. Hutchinson, M. B. Pepys, H. Boeing, R. Muche, H. Brenner and W. Koenig, *Diabetes Care*, 2000, **23**, 1835-1839.
25. S. F. Yang, B. Z. Gao, H. Y. Tsai and C. B. Fuh, *Analyst*, 2014, **139**, 5576-5581.
26. W. Fakanya and I. Tothill, *Biosensors*, 2014, **4**, 340.